Journal of Advances and Scholarly Researches in Allied Education
Vol. 13, Issue No. 2, July-2017, ISSN 2230-7540

Electronic Supporting Information [ESI] Formation and Chemistry of Carboxylic Anhydrides at the Graphene Edge

Praveen Kumar*

Professor

Abstract – Utilizing graphene for an extensive variety of uses regularly requires fragile substance handling and functionalization. Here we initially report the amalgamation of graphene nanoflakes with carboxylic corrosive gatherings at the graphene edges from multi-divider carbon nanotube materials. Utilizing this material we at that point demonstrate that exceptionally responsive carboxylic anhydride bunches exist in unique harmony with the carboxylic acids in watery scattering. Warming in vacuum moves the balance as around 80% of the carboxylic corrosive gatherings change to the anhydrides. These new bits of knowledge into graphene science empower us to build up a straightforward, straight-forward concoction functionalisation convention for graphene making utilization of the anhydrides. The graphene nanoflakes were found to respond promptly with amine nucleophiles in fluid scattering to yield the relating amides. The new convention enables us to change the zetapotential of the graphene nanoflakes and to enliven the graphene edges with gold nanoparticles. Because of its straightforwardness, we anticipate that this methodology will discover far reaching use in the compound functionalisation of graphene and to empower new graphene-based applications.

Keywords: Electronic Supporting Information[ESI], Carboxylic Anhydrides, and graphene edge

----------X----------

INTRODUCTION

Graphene, a solitary layer of graphitic carbon, shows profoundly amazing physical properties, for example, mechanical stability, optical transparency, impermeability, and electrical and thermal conductivity. Chemical handling and functionalisation are frequently required to utilize graphene in applications as differing as medication delivery, photovoltaic, and electronic devices, vitality stockpiling and synthetic sensors. The science of graphene is astoundingly mind boggling and a few angles, for example, the compound structure of graphene oxide, are even questionable. Graphene science can be partitioned as for the locus of compound functionalisation, i.e. either on the basal plane or at the edge which commonly depends on carboxylate science. Current standard techniques are carbodiimide-catalysedor continue through corrosive chlorides.

Our new arrangement system for cx-GNFs depends on the oxidative separate of CVD multi-divider carbon nanotube material in an initial step with a 3:1 vol% blend of concentrated sulfuric and nitric corrosive. The detachment of the cx-GNFs from the a lot of the inorganic acids is accomplished by balance with KOH pellets which prompts precipitation of K2SO4 and KNO3 while the cx-GNFs stay in scattering (Fig. 1b). The staying broke down salts in the cx-GNF scattering are then expelled by dialysis and the unadulterated cx-GNF material is acquired after stop drying in 16 w% yield (additionally subtle elements are given in the ESIf).

The virtue of the cx-GNFs is shown by the overview X-beam photoelectron range in Fig. 1c which demonstrates no different components than carbon and oxygen. A high-determination range of the C1s district affirms the nearness of sp2 carbon with a pinnacle focused at 285.3 eV and additionally a lower power top at 289.4 eV which is ascribed to carbon in oxidation state +III, for example, in carboxyl (COOH) gatherings.

SAMPLE CHARACTERIZATION

Optical absorbance spectroscopy

Optical absorbance spectra of fluid scatterings were recorded on a Perkin Elmer Lambda 900 spectrometer utilizing 1 cm quartz cuvettes and an output rate of 120 nm min-1.

1. X-Beam photoelectron spectroscopy (XPS)

All XPS estimations were done on a Thermo Logical K-Alpha XPS machine with a monochromated Al Ka source (£=1486.6 eV), a twofold centering 180 degree half of the globe analyser of ~ 125 mm range and identified with a 18 channel position touchy identifier. A double shaft surge weapon (electrons and argon particles) was utilized to make up for charge collection on the deliberate surfaces. All study examines were filtered 3 times with a determination of 1 eV, 400 pm spot size and 50 ms stay time. Every basic area were examined 10 times with a determination of 0.1 eV, 400 pm spot size and 50 ms stay time. The spectra were broke down with the Casa XPS programming.

2. Nuclear power microscopy (AFM)

For AFM examination, fluid cx-GNF scatterings (~0.1 mg mL-1) were dropped onto crisply separated 'profoundly arranged pyrolytic graphite' (HOPG) utilizing a Laurell Advances WS-650 turn coater (2000 rpm). A Computerized Instruments Multimode Nanoscope examining test magnifying lens with an IV Nanoscope controller made by Bruker was utilized for AFM estimation in the tapping mode utilizing the 'E' scanner. For naming artificially functionalised GNFs with Au nanoparticles, one drop of 5 nm Au nanoparticles scattered in 0.1 mM phosphate cradled saline arrangement was turn covered at 2000 rpm for 2 min onto a newly divided HOPG substrate as portrayed beforehand. The GNFs (one drop, ~0.1 mg mL-1) were then turn covered onto an indistinguishable substrate similarly from some time recently.

3. Strong state NMR spectroscopy

A Bruker Avance 300 spectrometer with 7.05 T wide-bore magnet at surrounding test temperature was utilized to play out all strong state 13C estimations. High-determination 13C strong state NMR spectra were recorded at 75.5 MHz with a Bruker 4 mm twofold reverberation enchantment point turning (MAS) test utilizing high-control proton decoupling (HPDEC). The working conditions were 13C 90°C heartbeat with a 3.7ps postponement; reuse deferral of 120 s with 908 drifters. The cx-GNFs and graphene oxide were pressed into zirconia rotors of 4 mm outside measurement and spun at 12 kHz MAS recurrence with a strength more noteworthy than ±3 Hz. The 13C concoction shifts are accounted for as for tetramethylsilane (TMS) which was aligned against a watery arrangement of 4,4-dimethyl-4-silapentane-1-sulfonic corrosive (DSS, 0 ppm), and glycine (176.46 ppm) individually.

4. Raman spectroscopy

All Raman estimations were done on a Renishaw Ramascope utilizing a 633 nm laser, 50-overlap amplification destinations, filter times of 20 seconds and gathering of 4.

5. Constricted aggregate reflectance infrared spectroscopy (ATR-IR)

FT-IR spectra were gathered on a Bruker Tensor 27 FTIR spectrometer utilizing the constricted aggregate reflectance infrared spectroscopy mode (ATR-IR) fitted with a room temperature DLaTGS locator at 4 cm-1 determination and a precious stone gem as the inside reflection component. A foundation range was permitted to keep running for 256 sweeps previously recording each example estimation which were then recorded for a similar time span.

6. Temperature customized desorption with mass spectrometry (TPD-MS)

2.5mg of the carbon nanomaterials were carbonized by warming from room temperature to 900°C at 10°C min-1 under high-vacuum conditions with a base weight of ~1.5 x 10-5 mbar utilizing a Carbolite MTF 1200 flat tube heater. The aggregate weight increments coming about because of desorbing gas were observed in-situ as a component of temperature utilizing a PTR225 cool cathode weight gage from Leybold. The idea of the vaporous species were examined with a HAL RC 201 mass spectrometer from Hiden Expository utilizing a Faraday Glass as the locator by filtering along the 1 to 200 a.m.u mass range each 5°C from room temperature to 900°C. Once the specimen achieved 900°C the carbonized material was cooled rapidly back to room temperature under vacuum before spilling to the environment and recouping the examples.

1.1 Zeta-potential measurements

1.2 All zeta potential measurements were carried out on a Malvern Zetasizer Nano (ZEN3600) machine using disposable Transmission electron microscopy

A JEOL JEM 2100 transmission electron magnifying instrument (TEM) with a Lanthanum hexaboride electron firearm with 200 kV electron vitality alongside a Gatan Orius camera was utilized to play out all TEM estimations. Before TEM imaging, tests were drop covered (2 drops, conc. »0.05 mg/mL) onto a copper matrix covered with fancy carbon.

2. READINESS OF CARBOXYLATED GRAPHENE NANOFLAKES (CX-GNFS)

2.1. Optimal response conditions for the readiness of cx-GNFs

C150P Baytube multi-divider carbon nanotubes (MWCNTs) arranged utilizing a CVD procedure by Bayer Materials Science (3 to 15 dividers of 5 to 20 nm external distance across, 2 to 6 nm inward measurement, 1 to 10 pm in lengths and free of indistinct carbon) were utilized as the beginning material for the readiness of the cx-GNFs. To streamline the yield and to limit the basal plane

oxidation of the cx-GNFs the impacts of response time and oxidation medium were examined. In particular, in an arrangement of analyses, 10 mg of the MWCNTs were ultrasonicated in 5 mL of either a 3:1 or a 1:1 vol% blend of conc. sulfuric corrosive (95-97% w/w) and conc. nitric corrosive (70% w/w) for 30 minutes. The response blends were then warmed at 100°C for variable measures of time, left to cool, weakened three-overlap with refined water and sifted through a 0.2 pm track-edged polycarbonate film. The ideal response time and conditions were controlled by measuring the absorbance of the filtrates at 500 nm (cf. Fig. S1). Two hours response time in the 3:1 vol% corrosive blend were distinguished as the ideal conditions.

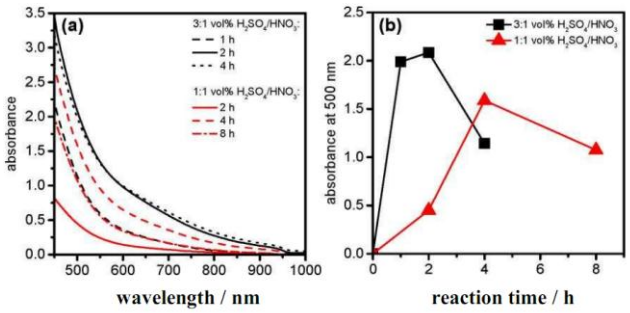

Figure S1 *(a) Optical absorbance spectra of the filtered reaction mixtures after oxidation in (i) 3:1 $H_2SOyHNO_3$ after 1 hour (black dotted), 2 hours (black solid) and 4 hours (black dashed) and (ii) 1:1 H_2SO_4:HNO_3 after 2 hours (red solid), 4 hours (red dashed) and 8 hours (red dot-dashed). (b) Absorbance values of the spectra in (a) at 500 nm.*

2.2 Large-scale preparation of cx-GNFs

Danger Cautioning. Concentrated sulfuric corrosive and nitric corrosive will be destructive and very oxidizing. Potassium hydroxide is exceedingly destructive and hygroscopic.

For an extensive scale arrangement of cx-GNFs, 500 mg of the MWCNTs were ultrasonicated in 250 mL of a 3:1 vol% blend of conc. sulfuric corrosive (95-97% w/w) and conc. nitric corrosive (70% w/w) for 30 minutes. The response blend was warmed at 100°C for two hours, left to cool and after that weakened threefold with refined water. The subsequent scattering was sifted through a 0.2 ^m track-edged polycarbonate film, the dark deposit on the layer was disposed of and the darker dark filtrate was killed by expansion of KOH pellets with outer ice shower cooling. After balance, a white salt accelerate was expelled by filtration (cf Fig. 1(b)) and the dark filtrate was amassed in vacuo. The scattering was first dialyzed against 1 M formic corrosive and afterward against high-virtue Milli-Q water utilizing SpectraPor 6 dialysis layers (MWCO 3.5 kDa). The advance of the dialysis was checked with a Mettler Toledo conductivity meter utilizing a Mettler Toledo LE703 conductivity sensor. The subsequent scattering was ignored a cation trade sap (Amberlite IR120, Sigma-Aldrich) and afterward solidify dried to give ~80 mg of dark colored dark cx-GNFs.

2.3 Amalgamation of cx-GNFs from Elicarb MWCNTs

Notwithstanding utilizing C150P Baytubes, we demonstrate that cx-GNFs can likewise be combined from Elicarb CVD MWCNTs (Thomas Swan Ltd). The XPS information beneath demonstrates the overview and C1s spectra of cx-GNFs got from Elicarb material utilizing a similar system nitty gritty above. In the accompanying, we will, in any case, utilize the cx-GNF material got from the Baytubes.

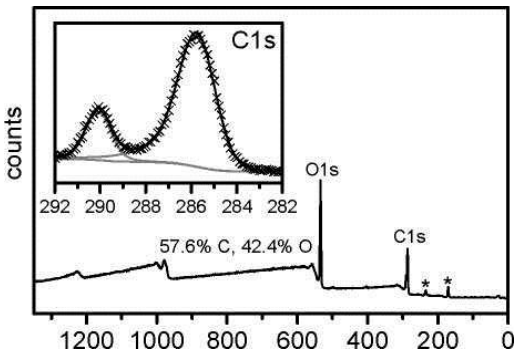

Figure S2. *XPS survey spectrum and C1s region of cx-GNFs synthesised from Elicarb MWCNTs. Asterisks indicate silicon dioxide contaminations arising from etched glassware.*

3. PREPARATION OF GRAPHENE OXIDE (GO)

Risk Cautioning. Potassium permanganate and sulfuric corrosive shape an exceptionally oxidizing blend which is conceivably dangerous within the sight of natural mixes, for example, CH3)2CO or ethanol. Hydrogen peroxide goes about as both a solid oxidizing and diminishing specialist. Correct control of temperature is central for the sheltered arrangement of GO.

For correlation of our cx-GNFs with another oxidized carbon nanomaterial GO tests were readied following a to some degree adjusted method by Chen et al.1 2 Graphite drops (1.00 g, > 100 work, Sigma-Aldrich) and concentrated sulfuric corrosive (25 mL, > 95 % w/w) were consolidated and blended at 0°C. Under incredible unsettling, potassium permanganate (3 g) was included gradually with the goal that the temperature of the response blend never surpassed

20°C. After this, the response blend was warmed at 40°C for 30 minutes. Refined water (50 mL) was then included and the arrangement blended for a further 15 minutes at 95°C. The dark colored blend was then weakened by expansion of 175 mL of water took after by dropwise expansion of 10 mL of 30% v/v hydrogen peroxide. The yellow-green blend was separated through a Whatman paper film, washed with 150 mL of 10% watery HCl and permitted to dry. The dry powder was scattered in 200 mL of refined water and dialyzed against a pre-treated standard grade, recovered cellulose dialysis film (Range Labs, MWCO 3.5 kDa). After dialysis, the graphite oxide was peeled by means of ultrasonication for a hour and a half. The scattering was then centrifuged at 3000 rpm for 40 minutes and emptied to disengage the peeled GO. The GO was then ultrasonicated afresh for 30 minutes and the scattering sifted through glass fleece. The filtrate was gathered and disregarded a cation trade pitch (Amberlite IR120, Sigma-Aldrich), focused and after that dried to give ~1 g of a darker powder.

4. SUBSTANCE FUNCTIONALISATION OF CX-GNFS

4.1. Synthesis of eth-GNF and cys-GNF

20 g of 5 wt % ethylenediamine or cysteamine in deionised water were added to 5 mg of cx-GNFs and the blends were permitted to respond for one hour at room temperature with incidental twirling. Hence, the dark colored scatterings of eth-GNF or cys-GNF were separated through a 0.2 pm Whatman polycarbonate layer to evacuate any hint of cross-connected drops. The filtrate was gathered, dialyzed against refined water and after that stop dried to yield the functionalised GNF materials.

4.2 Union of Al - GNFs

An answer of fluid aluminum chloride (10 mL, 0.1 M) was added to the cx-GNFs (10 mg) and the blend ultrasonicated for 10 min. After this, the aluminum-chelated GNFs (Al-GNFs) hastened out of scattering and were permitted to settle. The blend was ultrasonicated again and by and by the encourage shaped was permitted to settle. This ultrasonication and settling method was rehashed one further time. The blend was then separated under lessened weight through a 0.2 pm track-edged polycarbonate film. The Al-GNFs on the layer were washed with 3 x 10 mL deionised water to expel any overabundance aluminum chloride before being left to dry on the film under diminished weight.

4.3 FT-IR spectra of eth-GNFs and cys-GNFs

FT-IR spectra of eth-GNFs and cys-GNFs are appeared in Fig. S3. The fruitful substance functionalisations of the cx-GNFs can be seen from the loss of otherworldly force at around 1700 cm-1 where the C=O extending method of COOH is found (cf. Fig. 2(b)).

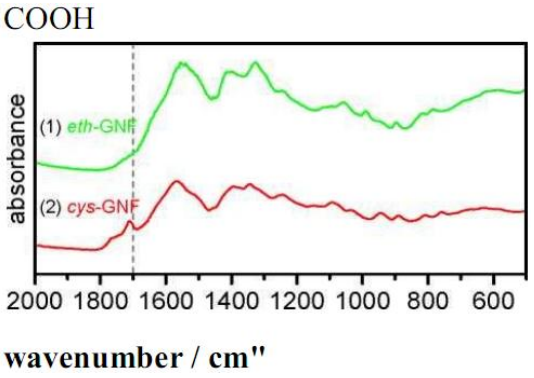

Figure S3. FT-IR spectra of (1) eth-GNFs and (2) cys-GNFs.

3.1 XPS spectra of eth-GNFs, cys-GNFs and Al-GNFs

The successful chemical functionalisation of the *cx*-GNFs can also been seen from the presence of nitrogen, sulfur and aluminium in the XPS survey spectra shown in Fig. S4.

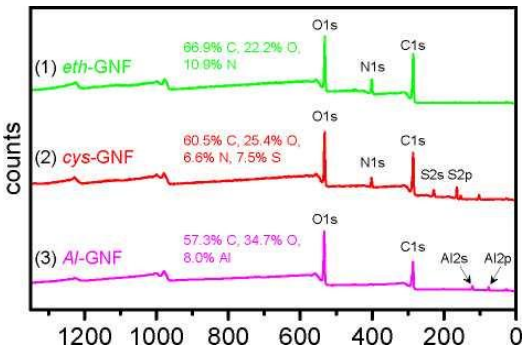

Figure S4. XPS survey spectra of (a) eth-GNFs, (b) cys-GNFs and (c) Al-GNFs.

The high-resolution spectra shown in Fig. S5 give additional information about the oxidation states of carbon, nitrogen and sulfur in the chemically functionalised *cx*-GNF samples. An additional peak in the C1s region of eth-GNF is found at around 286.6 eV which is attributed to the methylene (CH_2) carbon atoms. The N1s region of the eth-GNF sample shows two different nitrogen environments corresponding to amine as well as amide nitrogen. As expected, the C1s region for *cys*-GNF also shows a peak for methylene carbon at ~286.5 eV. The N1s and S2p regions show single oxidation states corresponding to amide nitrogen and thiol sulfur, respectively.

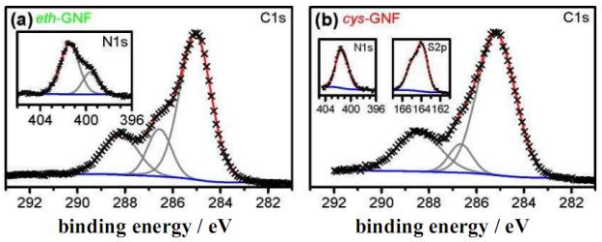

Figure S5. XPS spectra of (a) eth-GNF and (b) cys-GNF in the C1s region. The N1s and S2p regions are shown as insets. The crosses represent the experimental data, blue line the background, gray lines the fitted peaks and the peak sum is shown in red.

5. TPD-MS MEASUREMENTS

5.1 Detailed analysis of the H_2O and CO_2 desorption from cx-GNFs

Figure S6 shows the gas desorption patterns for H2O and CO2 from the data shown in Fig. 2(c) recorded upon heating *cx*-GNFs.

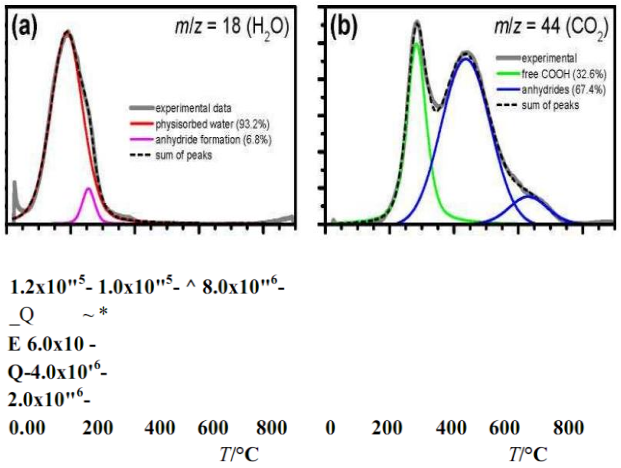

Figure S6. Thermal desorption patterns of cx-GNFs at (a) m/z=18 (H_2O) and (b) m/z=44 (CO_2). The area percentages of the individual components are given in the legend.

Pinnacle fitting with Pseudo-Voigt capacities demonstrates that around 93% of the desorbing H2O begin from physisorbed water. Steady with the FT-IR spectra appeared in Fig. 2(b) the loss of water because of anhydride arrangement begins at around 200°C. In general, just around 7% of the desorbing water from the cx-GNF test is because of anhydride development.

As indicated by the FT-IR investigation in Fig. 2(b) were allot the lower temperature CO2 desorption crest to the decarboxylation of 'stranded' COOH bunches which have not shaped anhydrides after warming. The decarboxylation from the anhydride bunches happens at higher temperatures and has a tail on the high-temperature side which we fit with an extra pinnacle. Generally, 67.4% of the desorbing CO2 start from the warm decay of anhydride gatherings and 32.6% are because of CO2 from 'stranded' COOH gatherings. Considering that two COOH bunches are expected to shape one anhydride assemble which then just discharges one likeness CO2 upon disintegration, we ascertain that exclusive around 19% of the COOH bunches in a cx-GNF test won't frame anhydrides after warming in vacuum.

5.2 Thermal gas desorption examples of GO

Notwithstanding the warm desorption information of cx-GNFs appeared in Fig. 2 we appear in Figure S7 the relating information for GO. As opposed to our cx-GNFs concurrent desorption of H2O, CO and CO2 is seen at around 250°C.

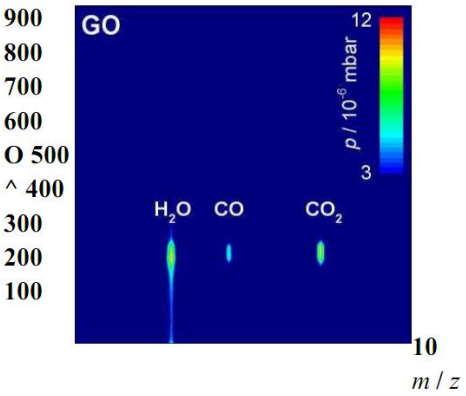

Figure S7. Thermal desorption pattern upon carbonizing 2.5 mg of GO.

6 Transmission electron microscopy (TEM) measurements

In addition to the AFM measurements shown the main article we have also characterised the dimensions of the *cx*-GNFs with TEM. The averages of the shortest and longest lateral diameters calculated from 17 flakes are 16 and 23 nm, respectively.

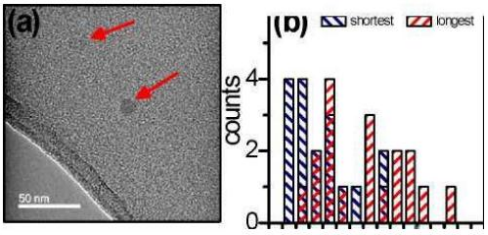

Figure S8. (a) TEM image of two cx-GNFs highlighted by arrows. (b) Diameter distribution of the cx-

7. STABILITY OF ANHYDRIDE-CONTAINING GNFS (AN-GNFS) IN WATER AND AIR

The chemical stability of the anhydride groups formed as a result of thermal desorption of H2O after heating cx-GNFs to 285°C was determined by dispersion of an-GNFs in water and exposing an-GNF powder to air. The FT-IR spectra in Fig. S8 show that the dispersion in water and exposure to air for 14 days reduced the amount of anhydride groups to the small amount that is present in the as-made material as well (cf Fig. 2(b)).

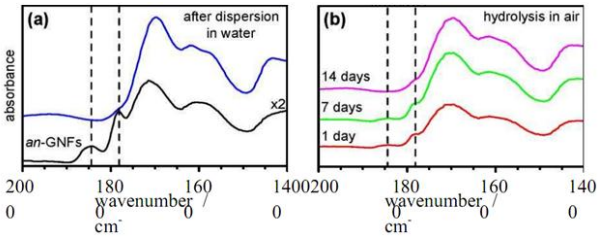

Figure S9. (a) FT-IR spectra of an-GNFs before (black) and after (blue) exposure to liquid water. (b) FT-IR spectra illustrating the hydrolysis of an-GNFs (black) to cx-GNFs upon prolonged exposure to air as indicated by the gradual decrease in the symmetric and asymmetric anhydride stretching modes centered at 1844 cm^{-1} and 1781 cm^{-1} (vertical dashed lines).

CONCLUSION

In rundown, we have opened up another section in graphene science by demonstrating that carboxylic anhydride bunches exist in unique harmony at profoundly carboxylated graphene edges. This was utilized to build up a straightforward single-step convention for compound functionalisation of graphene. We foresee that the new technique will be utilized broadly for, for instance, making graphene building obstructs for the advancement of new self-get together methodologies or connecting amine-containing biomolecules, for example, proteins or chemicals, to graphene for therapeutic and vitality related applications.

8. REFERENCES

A. M. Dimiev and T. A. Polson (2015). *Carbon,* 2015, **93**, pp. 544-554.

C. G. Salzmann, V. Nicolosi and M. L. H. Green (2010). *J. Mater. Chem.,* 2010, **20**, pp. 314-319.

C. K. Chua and M. Pumera (2013). Chem. Soc. Rev., 42, pp. 3222– 3233.

D. R. Dreyer, S. Park, C. W. Bielawski and R. S. Ruoff (2010). Chem. Soc. Rev., 39, pp. 228–240.

H. J. Salavagione, G. Mart´ınez and G. Ellis, Macromol (2011). Rapid Commun., 32, pp. 1771–1789.

H. J. Salavagione, J. Mater (2014). Chem. A, 2, p. 1738.

H. J. Salavagione, M. A. Gomez and G. Martinez (2009). *Macromo/ecu/es*, **42**, pp. 6331-6334.

H.-C. Chen, Y.-H. Chen, S.-L. Chen, Y.-T. Chern, R.-Y. Tsai and M.-Y. Hua (2013). Biosens. Bioelectron., 46, pp. 84–90.

J. Chen, B. W. Yao, C. Li and G. Q. Shi (2013). *Carbon,* 64, pp. 225-229.

J. L. Segura and H. J. Salavagione (2013). Curr. Org. Chem., 17, pp. 1680–1693.

J. P. Rourke, P. A. Pandey, J. J. Moore, M. Bates, I. A. Kinloch, R. J. Young and N. R. Wilson (2011). *Angew. Chem. Int. Ed.,* **50**, pp. 3173-3177.

L. Liao, H. Peng and Z. Liu (2014). J. Am. Chem. Soc., 136, pp. 12194–12200.

L. M. Veca, F. Lu, M. J. Meziani, L. Cao, P. Zhang, G. Qi, L. Qu, M. Shrestha and Y.-P. Sun (2009). *Chem. Comm.,* pp. 2565-2567.

L. Rodriguez-Perez, M. A. A. Herranz and N. Martin (2013). Chem. Commun., 49, pp. 3721–3735.

M. Castela´ın, G. Mart´ınez, C. Marco, G. Ellis and H. J. Salavagione (2013). Macromolecules, 46, pp. 8980–8987.

M. Quintana, E. Vazquez and M. Prato (2013). *Acc. Chem. Res.,* 2013, **46**, pp. 138-148.

S. Eigler and A. Hirsch, Angew (2014). Chem., Int. Ed., 2014, 53, pp. 7720–7738.

S. Niyogi, E. Bekyarova, M. E. Itkis, J. L. McWilliams, M. A. Hamon and R. C. Haddon (2006). *J. Am. Chem. Soc.,* 2006, **128**, pp. 7720-7721.

S. Sarkar, E. Bekyarova and R. C. Haddon (2012). Acc. Chem. Res., 45, pp. 673–682.

S. Sarkar, E. Bekyarova, S. Niyogi and R. C. Haddon (2011). J. Am. Chem. Soc., 133, pp. 3324–3327.

W. S. Hummers and R. E. Offeman (1958). *J. Am. Chem. Soc.,* 1958, 80, pp. 1339-1339.

X. Jia, J. Campos-Delgado, M. Terrones, V. Meuniere and M. S. Dresselhaus (2011). *Nanosca/e,* **3**, pp. 86-95.

Y. Xu, Z. Liu, X. Zhang, Y. Wang, J. Tian, Y. Huang, Y. Ma, X. Zhang and Y. Chen (2009). *Adv. Mater.,* **21**, pp. 1275-1279.

Z. Liu, J. T. Robinson, X. Sun and H. Dai (2008). *J. Am. Chem. Soc.,* 2008, **130**, pp. 10876-10877.

Corresponding Author

Praveen Kumar*

Professor

E-Mail – ashishkumar1982@outlook.com